Magazine of Civil Engineering

ISSN 2712-8172

journal homepage: http://engstroy.spbstu.ru/

Research article

UDC 69.01

DOI: 10.34910/MCE.124.2

Concrete face rockfill dam located on deformed foundation: stress-strain state

M.P. Sainov ✉

Moscow State University of Civil Engineering (National Research University), Moscow, Russian Federation

✉ *mp_sainov@mail.ru*

Keywords: dams, concrete face rockfill dam (CFRD), cutoff wall, stress-strain state, finite element method, soil foundation, numerical modelling

Abstract. Concrete face rockfill dam (CFRD) located on soil foundation has a composite structure of the seepage control facility. It includes three elements: the dam concrete face, the seepage control cuttoff wall (CW) in the foundation and the concrete apron connecting them. There is an urgent task to study workability and stress-strain state (SSS) of the seepage control facility as a whole structure as well as each element separately. Method. The SSS analysis of an abstract dam with the aid of numerical modeling was conducted to solve this task. A 100 m high CFRD located on a 100 m thick foundation layer was considered. Analyses were conducted for several alternatives of foundation soils with deformation modulus from 40 to 5000 MPa. Results. The analyses showed that the SSS of the dam on the soil foundation drastically differs from the SSS of the dam on the rock foundation. The concrete face and the cuttoff wall are subject to considerable compressive longitudinal forces. Due to bending deformations in CW and the concrete apron, considerable tensile stresses may occur. Conclusions. A number of recommendations was formulated for providing strength of the elements of the composite seepage control facility of the dam on soil foundation. To provide strength of the concrete face it is necessary that the deformability of the dam soil be close to the foundation soil. To provide CW with strength, it is recommended use the material with rigidity of no more than by 2–3 times greater than the foundation soil rigidity. The most vulnerable element of the structure of the composite seepage control facility is the concrete apron. To avoid cracking in it, it should be cut by transversal joints to form separate slabs.

Citation: Sainov, M.P. Concrete face rockfill dam located on deformed foundation: stress-strain state. Magazine of Civil Engineering. 2023. Article no. 12402. DOI: 10.34910/MCE.124.2

1. Introduction

Concrete face rockfill dam (CFRD) is one of the embankment dam types, which may be used practically in any conditions, where stone is available for the dam body.

The classic structure of CFRD used from the end of the 20th century is built on rock foundation. It includes 2 elements: a concrete face and a concrete apron. A concrete face (CF) covering the upstream face is made thin-walled and is uncut vertically. A short concrete apron is located on the foundation surface from where the grout curtain in rock foundation is fulfilled. CF and the apron are separated from each other by a perimeter joint. It has a movable connection; it is made in a way of providing potential deflections and other displacements of the face relative to the apron.

If a CFRD is located on soil (deformed) foundation, its structural design is similar to the classic one, however, it has its specific features. The main difference is the presence of the cutoff wall (CW) in the foundation to prevent seepage. CW joins the upstream face of the apron forming a unified seepage control

contour (Fig. 1). Thus, a CFRD on soil foundation has a seepage control facility (SCF) of a composite structure. It includes not two but already three elements.

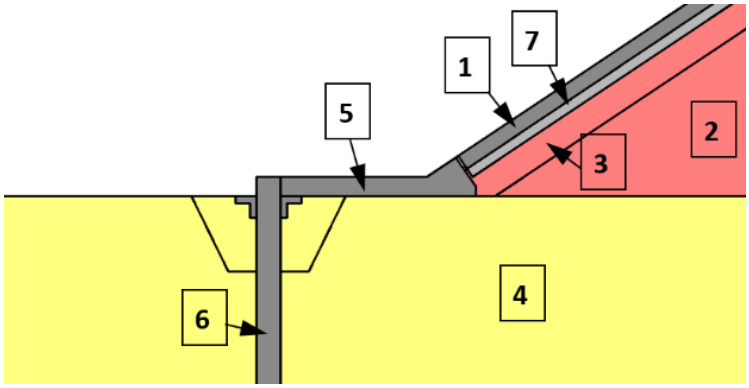

Figure 1. Diagram of the interface of the seepage control facility elements: 1 – reinforced concrete face; 2 – rockfill dam shell; 3 – supporting zone; 4 – foundation layer; 5 – concrete apron; 6 – cutoff wall in the foundation; 7 – lean concrete layer.

CFRDs located on a foundation deformed layer are rather popular. Parameters of such dam structural designs are listed in [1–6]. Alto Anchicaya dam 154 m high built on soil foundation may be considered the first ultra-high CFRD of modern structural design. This dam was constructed in 1983 in Columbia on a 34 m thick layer of sand and gravel.

In the 21st century, a number of CFRDs were constructed on soil foundation. At their listing we will indicate their height H and thickness of soil deposits layer T. The list contains the following dams: Dhauliganga (2006, India, H = 56 m, T = 70 m), Aertash (Turkey, H = 164.8 m, T = 94 m) [1], Limon (Chili, H = 82 m, T = 46 m) [7], Nalan (2005, China, H = 109 m, T = 24 m) [8], Jiudianxia (2008, China, H = = 136.5 m, T = 56 m) [9], Chahanwusu (2009, China, H = 107.6 m, T = 47 m) [10], Miaojiaba (2011, China, H = 111 m, T = 48 m) [2, 11].

The highest CFRD on soil foundation is Aertash dam in Turkey; it was constructed on a layer of alluvial soils [1]. Its CF is from 0.4 to 1 m thick, with the 1.2 m thick CW. The CW is made of reinforced concrete.

In 2014, a dam received a CW providing water tightness not only of the foundation but also of the lower part of the dam for the first time [12, 13]. It is the 140 m high Arkun dam constructed in Turkey. Such a structure may be considered as a perspective type of CFRD refinement.

However, in order to use the structural designs of the dams with composite seepage control elements it is necessary to be assured in their safety and tightness of the elements interface. At that, it is necessary to take into account that the composite seepage control facility works in other conditions as compared to the classic structure of CFRDs located on the rock foundation.

A number of foreign publications are dedicated to stress-strain state (SSS) analyses of CFRDs located on deformed foundation. Some publications [8–10, 14] are dedicated to determination of the dam and foundation deformations, while neglecting the strength of the seepage control facility elements in them.

A large scope of investigations was carried out by Chinese specialists [2, 3, 12]. With the aid of 3D numerical modeling of SSS and field observations over deformations and stresses at constructed Miaojiaba dam they studied SSS of CW integrated in the composite SCF. However, CF strength was not estimated. Besides, these investigations were conducted only on the example of one particular structure.

In order to study workability of composite SCF of the dam on deformed foundation we carried out methodical investigation of the foundation properties' effect on SSS. Some preliminary results have been published earlier in [15].

Assessment of workability of seepage control facility of CFRDs located on soil (deformed) foundation is an urgent issue. For this purpose, it is necessary to carry out SSS analyses of such dams.

These analyses should solve the following issues:

Issue No. 1. Workability of the elements of traditional CFRD structure at its location on the deformed foundation. How does the foundation deformation affect SSS and strength of the concrete face and the concrete apron?

Issue No. 2. Workability of the CW interface with the concrete apron. Is the interface between CW and the concrete aprons still tight?

2. Materials and Methods

In the study, we considered an abstract 100 m high rockfill dam located on a 100 m thick layer of the deformed foundation (Fig. 2).

The structure of the dam is as follows. The dam slopes are 1:1.7. On the upstream slope of the dam there is a concrete face (CF) of variable thickness (from 0.3 m on the top to 0.8 m at the toe). The face is placed on the lean concrete supporting zone [16, 17], which is called “extruded curb” or “extrusion-sidewall” (SW). Deformation modulus of lean concrete is approximately 5000 MPa [18]. A thin layer of mastic is placed between the face and the supporting zone, which is intended for decreasing friction in compliance with the bond-breaking concept used for structures of modern CFRDs [19].

The wall in the foundation is 1.2 m thick. It is connected with the face by an apron 10 m long and 1 m thick.

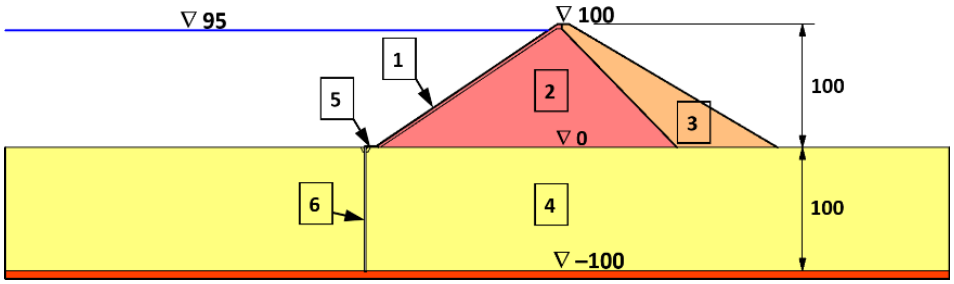

Figure 2. Diagram of concrete face rockfill dam located on deformed foundation layer: 1 – reinforced concrete face; 2 and 3 – upstream and downstream parts of the shell of the rockfill dam; 4 – foundation layer; 5 – concrete apron; 6 – seepage control wall in the foundation.

SSS analyses of the structure were carried out by the finite element method with the aid of the author’s computer program NDS_N. Analyses were conducted in 2D formulation.

The dam and the foundation were divided into 1220 solid finite elements and 76 contact finite elements (Fig. 3). The contact elements modeled had non-linear character of the interface between soils and rigid constructions. In order to simulate a complicated character of SSS of rigid thin-walled constructions we used finite elements with cubic power of displacements approximation. The total number of freedom degrees of the finite element model amounted to 11852.

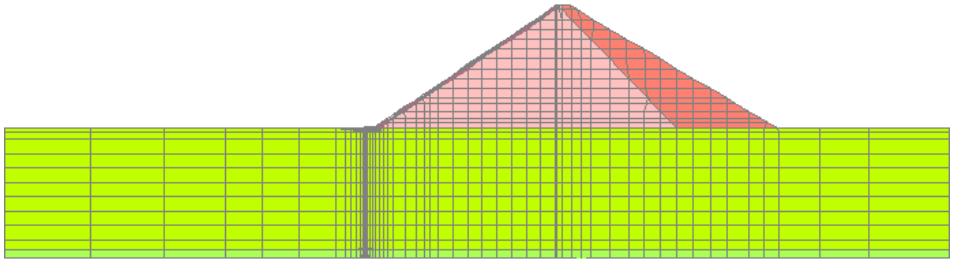

Figure 3. Diagram of finite element discretization of the structure.

The study was conducted for several combinations of the dam and foundation soil deformation properties.

We considered two alternatives of the dam body rockfill (rock mass). In the first alternative (alternative A) the rockfill modulus of linear deformation E_{d1} of the dam upstream was assumed to be equal to 120 MPa, and in the second (alternative B) it was 480 MPa. The modulus of linear deformation of rockfill in the downstream part of the shell was taken 2 times less than that of the upstream part.

In addition, we considered four alternatives of foundation soil types and, accordingly, characteristics of foundation deformation. Alternatives “a” and “b” correspond to soils of gravel-pebble, alternatives “c” and “d” to rocks. Alternative “a” approximately corresponds to foundation soils of Aertash dam [1], and alternative “d” corresponds to soils of Karkhe dam [20].

Mechanical properties of foundation soils are presented in Table 1. The table also indicates the strength indices of foundation soils by Mohr-Coulomb model. For rockfill, the angle of internal friction was taken equal to 47°.

The cutoff wall material was assigned depending on deformability of foundation soils. It was assumed that deformation modulus of the wall material should not exceed the deformation modulus of the foundation soil by more than 5 times (Table 1). We chose cast clay-cement concrete for alternative “a”; plastic concrete

for alternatives “b” and “c”; concrete for alternative “d”. The CW measurements data for Karkheh dam show plastic concrete has deformation modulus of approximately 500–2000 MPa and compressive strength of 2–3.5 MPa [20, 21]. The CW measurements data for Kureika dam suggest the cast clay-cement concrete has deformation modulus 30–200 MPa, and its uniaxial compressive strength comprises 1–2 MPa [22].

In total, we considered eight design alternatives with various combinations of the dam and foundation material (Table 1). Alternatives “A.d” and “B.d” correspond to the case of using the traditional structural design of CFRD on rock foundation.

Table 1. Mechanical properties of materials in design alternatives.

Alternative No.	Dam			Foundation				CW	
	E_{d1} [MPa]	E_{d2} [MPa]	ν_n	E_o [MPa]	ν_o	φ_o	c_o [kPa]	E_c [MPa]	ν_c
A.a	120	60	0.2	40	0.33	38	0	200	0.33
A.b	120	60	0.2	200	0.33	40	0	1000	0.30
A.c	120	60	0.2	1000	0.33	30	30	5000	0.25
A.d	120	60	0.2	5000	0.25	33	50	29000	0.20
B.a	480	240	0.2	40	0.33	38	0	200	0.33
B.b	480	240	0.2	200	0.33	40	0	1000	0.30
B.c	480	240	0.2	1000	0.33	30	30	5000	0.25
B.d	480	240	0.2	5000	0.25	33	50	29000	0.20

Designations: E_{d1}, E_{d2} are rockfill modulus of linear deformation in the upstream and downstream parts of the dam respectively; E_o, E_c are module of linear deformation of the foundation soil and the wall material respectively; ν_n, ν_o, ν_c are Poisson’s ratios of rockfill, foundation soil and the wall material respectively; φ_o, c_o are the angle of internal friction and specific cohesion of foundation soil respectively.

For the face concrete, the modulus of linear deformation was taken equal to 29000 MPa, Poisson’s ratio was 0.2.

Computation was conducted for loads of dead weight and hydrostatic pressure acting on the upstream faces of seepage control facilities. It was assumed that SCF fully cuts through the impervious foundation layer and reaches headwater. Therefore, SCF is subject to total hydrostatic pressure from the upstream and downstream sides.

SSS analyses were carried out with consideration of the dam construction and the reservoir impoundment sequence. The following staged diagram was assumed. At the first stage, we modeled the formation of the foundation SSS, then arrangement of SCF in it. During the following 15 stages, we modeled layered dam filling by horizontal layers. Only after that the face was “placed” for the full height. Then gradual reservoir impoundment was modeled with growth of hydrostatic pressure on the upstream part of the face, the apron and the wall.

3. Results and Discussion

The dam SSS analysis for all the considered alternatives was fulfilled until the level of the reservoir impoundment reached the elevation of 95 m. The analysis was conducted for the following parameters: displacement of the dam and the foundation, displacements of the upstream part of the face and CSF, stresses in the dam body and the foundation, stresses on the upstream and downstream faces of CF. The distribution of displacements and stresses is shown in Fig. 4–14, and their maximum values are in Table 2.

Table 2. Parameters of the dam SSS for design alternatives.

Alternative No.	Dam	Foundation	Dam SSS		Concrete face SSS			Wall SSS		
	E_{d1} [MPa]	E_o [MPa]	U_x [cm]	U_y [cm]	U_n [cm]	max σ_n [MPa]	min σ_n [MPa]	U_x [cm]	min σ_y [MPa]	max σ_y [MPa]
A.a	120	40	179	311	186.8	–	-9.6	161	-6.1	0.3
A.b	120	200	50	72	47.3	–	-7.6	35	-4.7	-0.2
A.c	120	1000	23.8	41	24.8	–	-3.1	9.6	-4.8	0.6
A.d	120	5000	18.2	37	20.7	0.3	-2.0	3.1	-4.3	–
B.a	480	40	185	307	172.8	2.1	-10.7	117	-6.4	0.4
B.b	480	200	36	61	36.2	–	-7.2	28	-4.9	-0.2
B.c	480	1000	11.1	15.8	10.5	–	-4.2	8.2	-4.9	-0.3
B.d	480	5000	5.7	10.2	6.2	–	-2.0	3.0	-4.5	0.2

3.1. Analysis of the dam and foundation displacements

Displacements of the computational domain over the construction period for different alternatives are shown in Fig. 4 (settlements U_y) and Fig. 5 (horizontal displacements U_x). Displacements of the foundation from its dead weight are not taken into account.

The analysis shows that the considered alternatives of the foundation and the dam properties greatly differ by value and character of the dam displacements' distribution.

In case of rigid rock foundation (E_o = 5000 MPa) the zone of maximum settlements U_y is located in the center of the dam body (Fig. 4, c, d), and in case of soil foundation (E_o = 40 MPa) it is located at the dam toe (Fig. 4, a, b). Maximum values of the structure settlements during construction in these alternatives differ approximately by an order of magnitude.

Maximum horizontal displacements U_x in most of the alternatives are observed on the dam upstream face (Fig. 5). Only in case of deformed foundation (in alternatives of series "a") the zone of high horizontal displacements is also located on the boundary between the dam and the foundation (Fig. 5, a, b). In this case the maximum dam displacement is approximately 30 times greater than that of rock foundation.

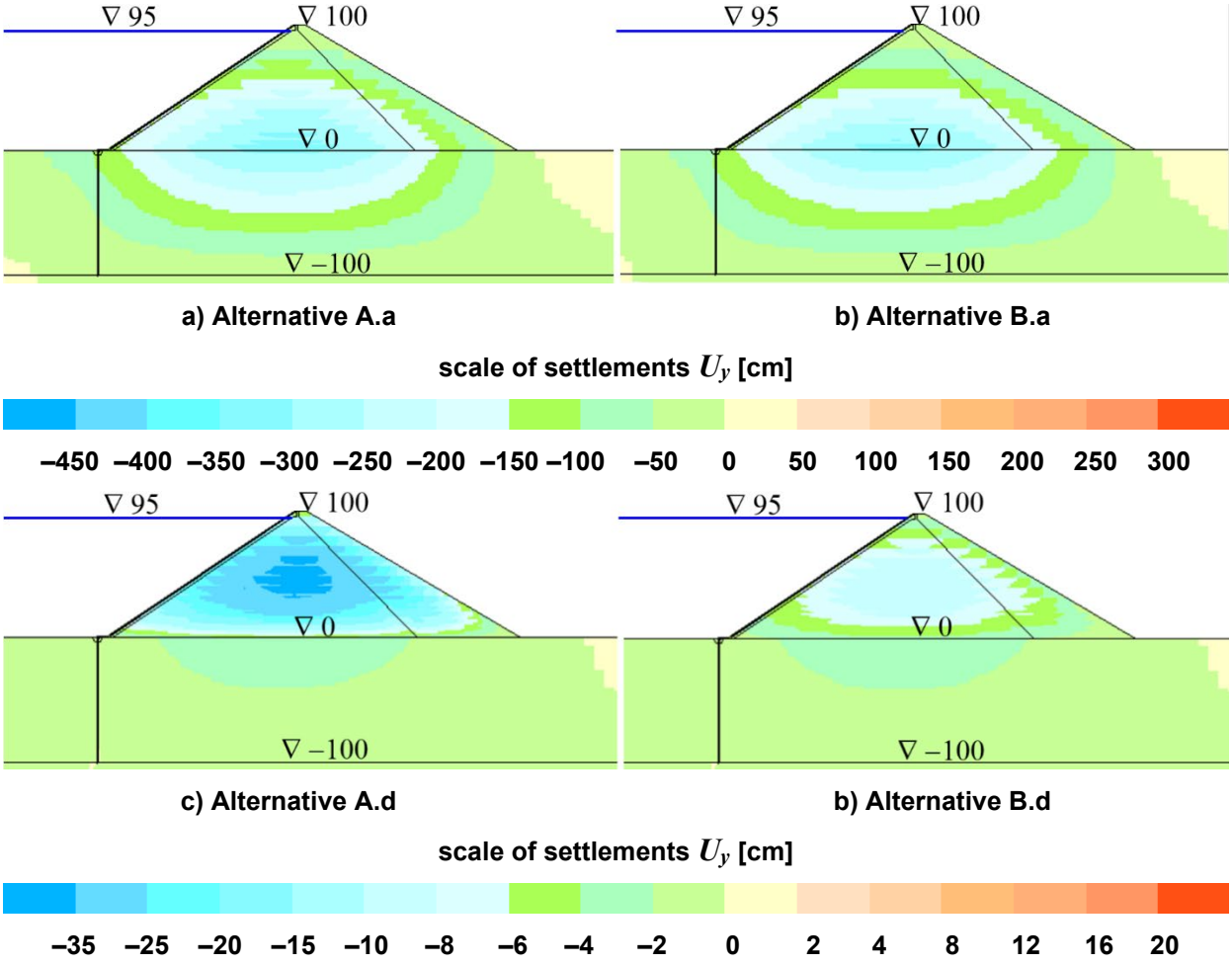

Figure 4. Distribution of the structure settlements in different alternatives: a, b – at E_o = 40 MPa; c, d – at E_o = 5000 MPa; a, c – at E_{d1} = 120 MPa; b, d – at E_{d1} = 480 MPa.

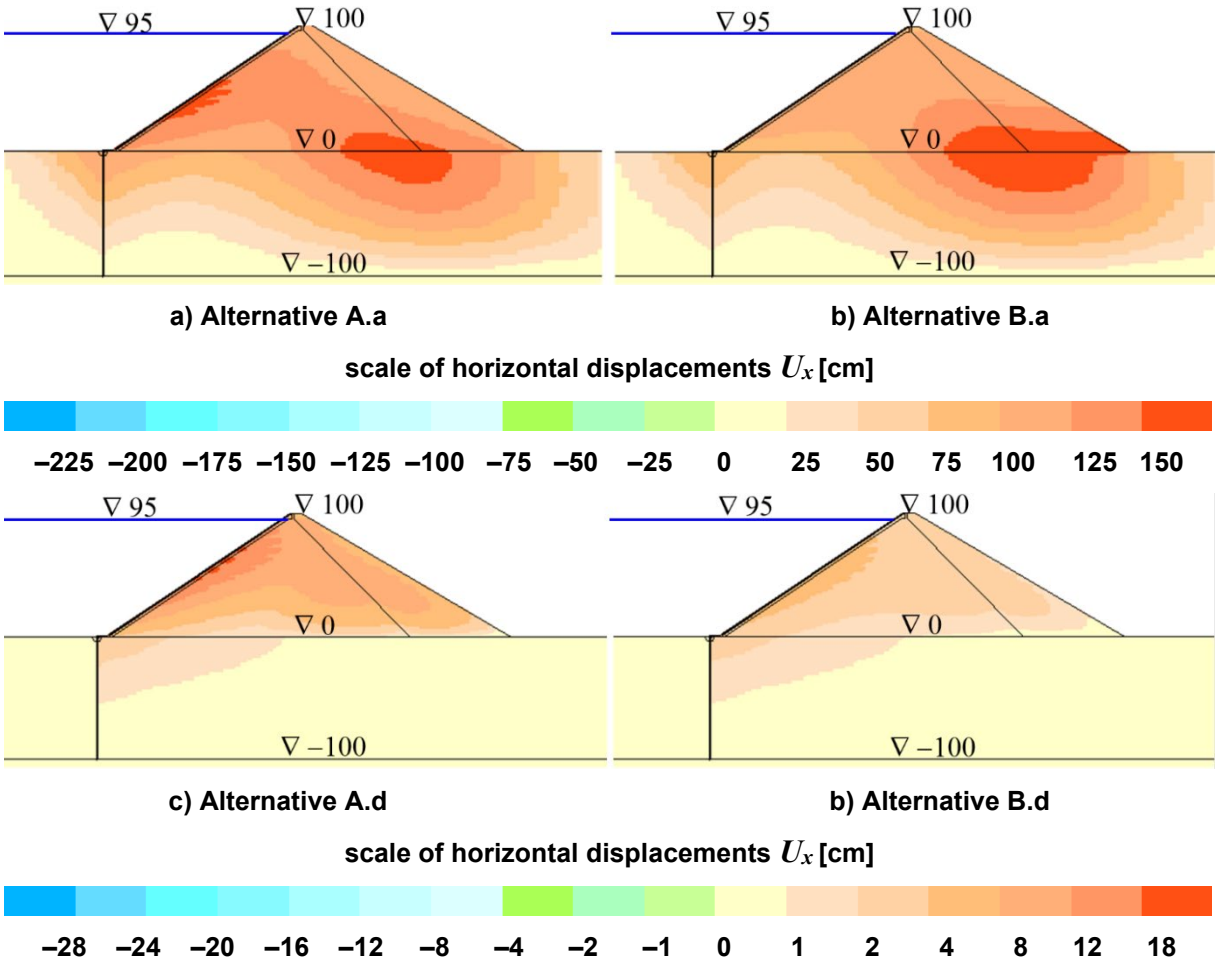

Figure 5. Distribution of the structure horizontal displacements in different alternatives: a, b – at E_o = 40 MPa; c, d – at E_o = 5000 MPa; a, c – at E_{d1} = 120 MPa; b, d – at E_{d1} = 480 MPa.

3.2. Analysis of stresses in the dam and foundation

Distribution of axial normal stresses σ_y and σ_x is shown in Fig. 6 and 7 respectively. The stresses presented in the figures do not take into account the stresses from the foundation dead weight.

The value and the character of distribution of vertical stresses σ_y slightly depend on the foundation deformation (Fig. 6). Stresses in the dam uniformly increase from the crest to the toe. In the upper part of the dam, the stresses σ_y are somewhat higher than in the downstream due to hydrostatic pressure on the face. In the foundation the compressive stresses actually do not vary depth wise.

In the zone of SCF arrangement, the stresses σ_y are relatively not high. In the downstream part from the wall the compression level slightly increases and in upstream part the stresses σ_y actually drop to 0 (Fig. 6).

With respect to stresses σ_x, the soil from the upstream side of the wall has deficit of compressive stresses and from the downstream part, there is additional compression due to hydrostatic pressure on the wall (Fig. 7).

The value and the character of distribution of horizontal stresses σ_x are greatly dependent on the ratio between deformation properties of the foundation and the dam body. The alternatives, where deformation moduli of the foundation and the dam considerably differ from each other, are characterized by considerable differences in the values of stresses σ_x between the dam body and the foundation.

At E_o >> E_{d1} (rigid rock foundation), a characteristic concentration zone of compressive stresses σ_x forms in the upper part of the foundation (Fig. 7,c,d); thus, the dam body soil has deficit of compressive stresses.

At E_o < E_{d1} (deformed soil foundation), a characteristic zone of soil shear strength loss forms in the lower part of the dam (Fig. 7,a,b). If during the analysis the soil is considered to be elastic, the tensile

stresses σ_x appear in this zone. As our calculations allowed for the fact that the soils had tensile strength, the tensile stresses would not occur and the soil is subject to loosening deformations. Tensile deformations result in additional settlements and displacements of the structure.

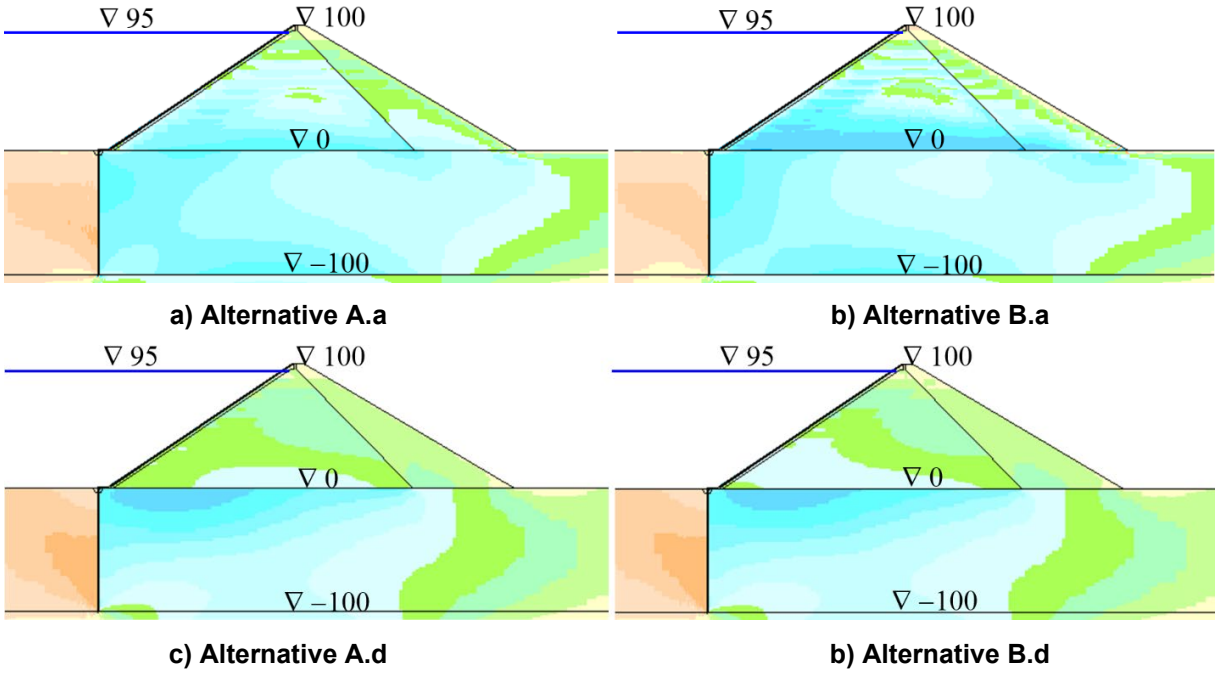

Figure 6. Distribution of horizontal stresses σx in different alternatives: a, b – at E_o = 40 MPa; c, d – at E_o = 5000 MPa; a, c – at E_{d1} = 120 MPa; b, d – at E_{d1} = 480 MPa.

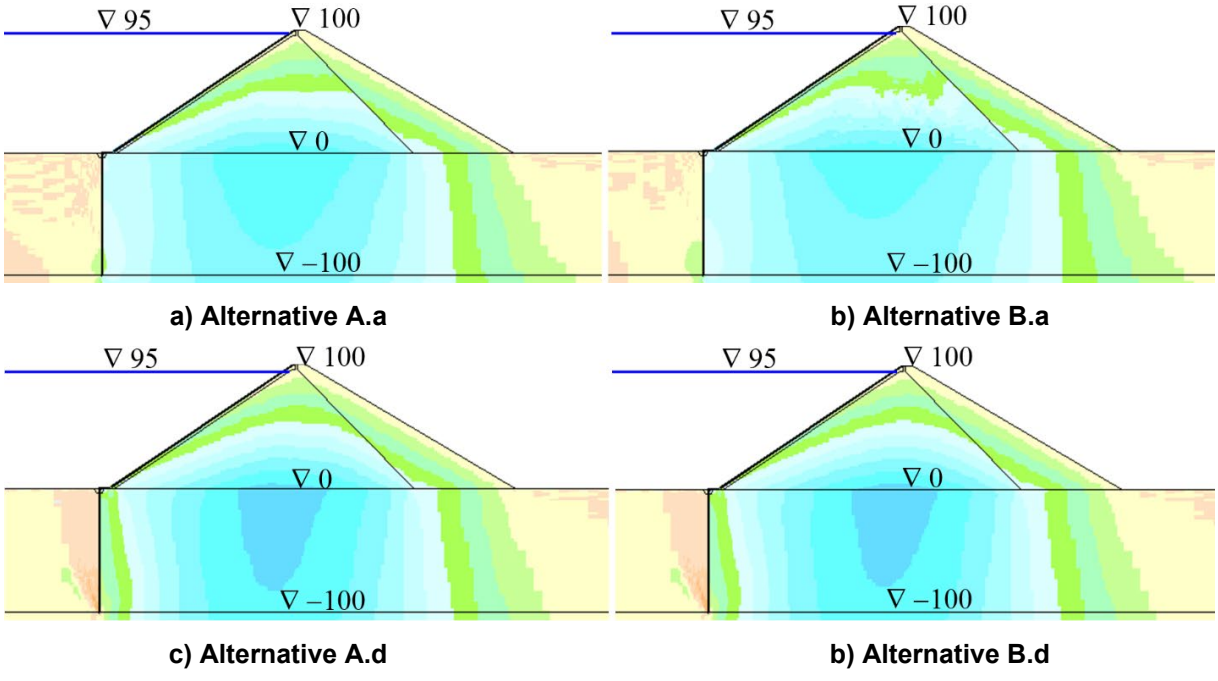

Figure 7. Distribution of horizontal stresses σ_y in different alternatives: a, b – at E_o = 40 MPa; c, d – at E_o = 5000 MPa; a, c – at E_{d1} = 120 MPa; b, d – at E_{d1} = 480 MPa.

3.3. Displacements of cutoff wall (CW)

In the same way as the displacements of the whole structure, displacements U_x of the wall are directed toward the downstream side. They have nearly uniform distribution heightwise and reach maximum at the wall head (Fig. 8). The displacements cause bending deformations at certain parts of the wall. Wall bending occurs at the section of thrust into the rigid apron and at conjugation with the rock foundation.

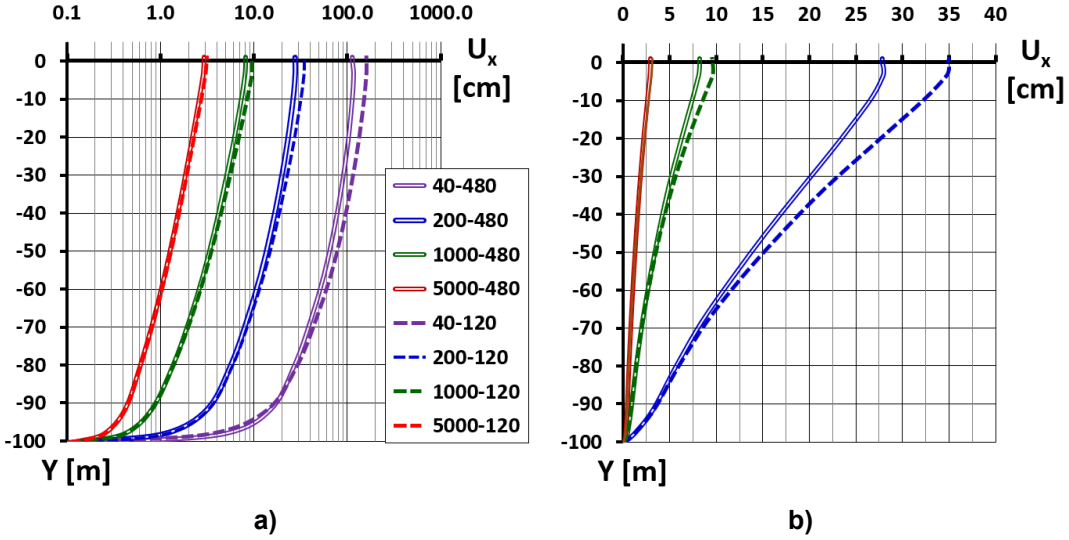

Figure 8 Displacements of the wall made in the foundation of variable rigidity. In the designation of the alternatives the first number indicates deformation modulus of foundation soil (MPa), the second number is deformation modulus of the dam soil (MPa): a – in logarithmic scale, b – in natural scale.

3.4. Analysis of concrete face displacements

Displacements of CF are shown in Fig. 9 in the form of its deflections, i.e. displacements in the direction perpendicular to the upstream face.

For the rigid foundation (alternatives of series “d”) the non-uniform distribution of the face deflections height wise is typical (Fig. 9). It provides evidence of deformations of the face transverse bending. Actually, height wise the face deflects toward the downstream side except for the top most part. At rigid foundation the maximum of value displacements and settlements are observed approximately at ∇45 m.

The higher the foundation deformation, the greater the face deflections. Deflections increase face height wise, but they are more intense near the dam toe (Fig. 9). In case of the soil foundation the face maximum deflections are observed specifically near the dam toe.

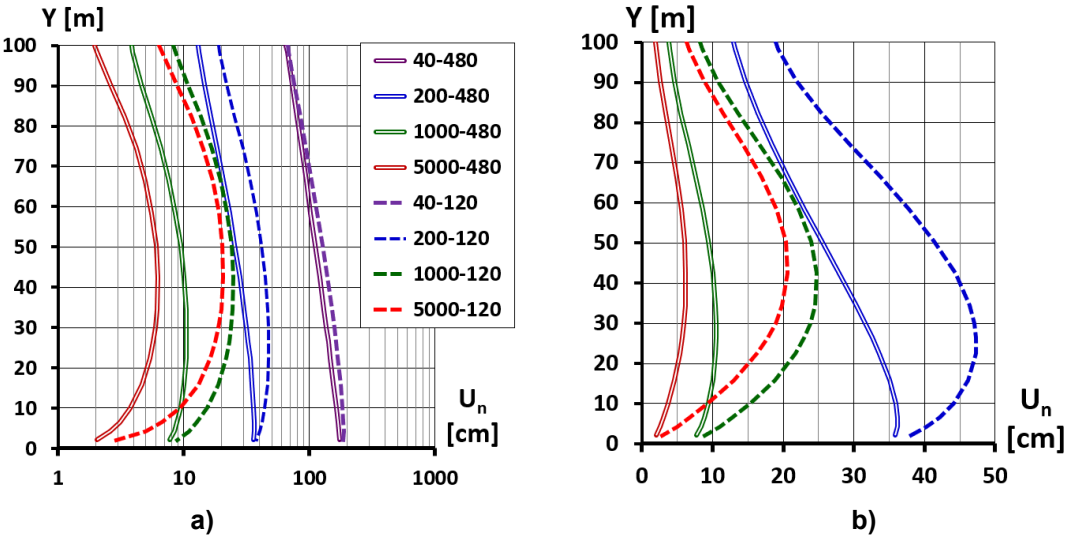

Figure 10. Height wise distribution of face deflections. In the designation of the alternatives the first number indicates deformation modulus of foundation E_o (MPa), the second number is deformation modulus of rockfill E_{d1} (MPa): a – in logarithmic scale, b – in natural scale.

Analysis of maximum values of the face deflections $U_{n,max}$ (Table 2) permits making the following conclusions:

- At rigid (rock) foundation (E_o > 1000 MPa) the maximum value of deflection slightly depends on deformation modulus of the foundation E_o and is mainly determined by deformation modulus of rockfill E_d.
- At soil foundation (E_o < 200 MPa) the maximum value of deflection actually does not depend on the dam rockfill deformation and mainly depends on deformation modulus of foundation E_o.
- At most deformed soil foundation (alternatives of series “a”) CF deflections amount to more than 1 % of the dam height.

3.5. Concrete face stress state

As it is known from the results of numerical modeling, CF stress state is formed not only due to deformations of transverse bending, but also due to longitudinal deformations [23, 24]. Analyses show that the lower part of the dam face on rock foundation may be subject to tensile longitudinal force.

Similar results were obtained for the alternatives of series “d” (E_o = 5000 MPa). Figs. 11, 12 show CF heightwise distribution of stresses σ_E, directed along the slope, i.e. longitudinal stresses. Fig. 11 shows stresses on the upstream and downstream parts of the face, and Fig. 12 shows average values of stresses (axial stresses).

As on the most part of the face length the bending is represented weakly, the stresses on its parts are close to each other. Only in the zone of conjugation with the apron, there is additional compression due to bending on the face upstream part, and on the downstream part, the compression decreases.

The value and the character of stresses’ distribution in CF depend on deformation of the foundation and the dam soils. The more the difference in deformation between the foundation and the dam is, the more the value of both average longitudinal stresses and irregularity of their distribution is.

In the alternatives of the dam on the rigid foundation (alternatives of series “d”), tensile stresses σ_E occur in the lower part of the face (Fig. 11, 12).

In the alternatives of the dam on the soil foundation (alternatives of series’ “a”, “b”), high compressive longitudinal stresses in the face are typical. Average compressive stresses reach approximately 9 MPa (Fig. 12). Maximum compression is observed at the height of 30 m. Compressive strength of the face concrete is provided if concrete of grade B30 is applied.

However, in case of soil foundation in the face beside compressive there may also occur tensile longitudinal stresses. Such effect was obtained in alternative B.a, where the dam deformation modulus was 12 times greater than the foundation deformation modulus. This alternative indicates considerable tensile stresses (Fig. 11, b), which exceed the tensile strength of B30 concrete (1.1–1.75 MPa).

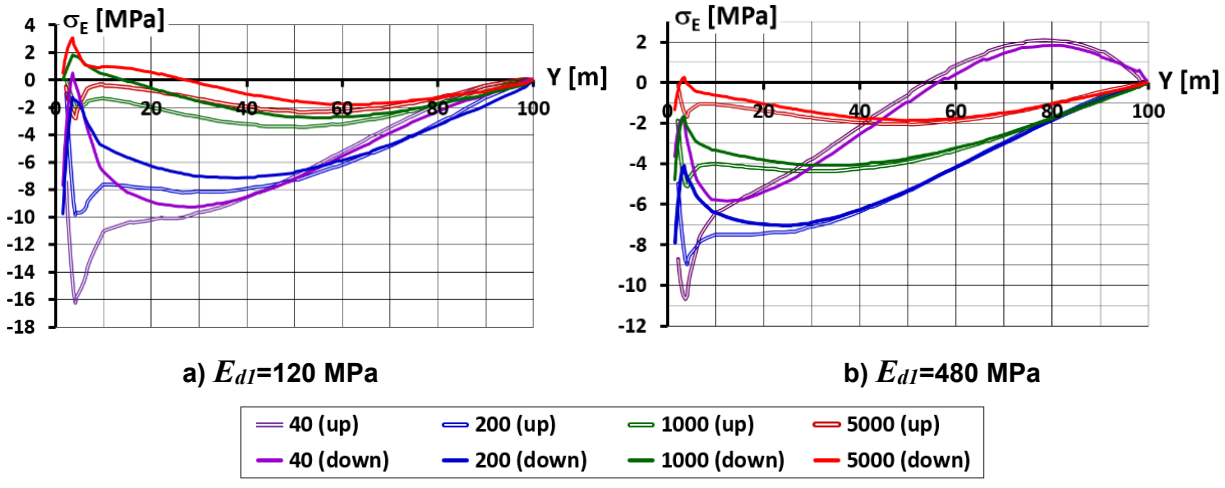

a) E_{d1}=120 MPa **b) E_{d1}=480 MPa**

Figure 11. Face height wise distribution of longitudinal stresses on the upstream and downstream sides. Designations indicate the value of deformation modulus of the foundation (MPa) and the face side.

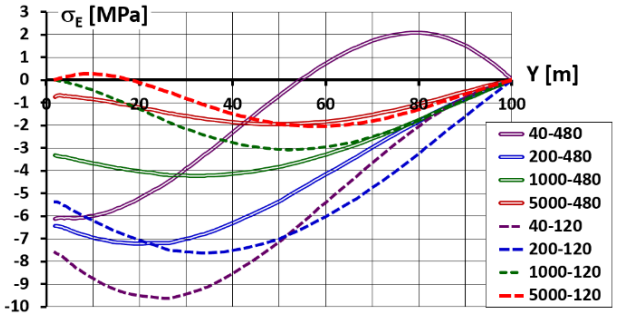

Figure 12. Face height wise distribution of average longitudinal stresses.

In alternative A.a, where the dam deformation modulus is only 3 times greater than the foundation deformation modulus, this effect is not observed. Thus, in CFRD on soil foundation there is a danger of strength loss of the face concrete.

3.6. Wall stress state

Fig. 13 shows average by the wall thickness vertical stresses σ_y for all the alternatives. For all the alternatives it is typical that the wall is subject to over compression in vertical direction. This effect is known from the results of field measurements and numerical modeling of CW SSS in foundations of high embankment dams [5, 15].

Excess of compressive stresses is related to the fact that the wall material is more rigid than the foundation soil. It occurs due to friction of soil settling relative to the wall. Compression stresses increase depth wise.

At most of the wall sections the stresses on the upstream and downstream faces of the wall are approximately similar. At the sections of conjugation of the wall with the rock foundation and with the apron, bending deformations cause the zones of concentration of compressive stresses and sometimes of tensile stresses (Fig. 13).

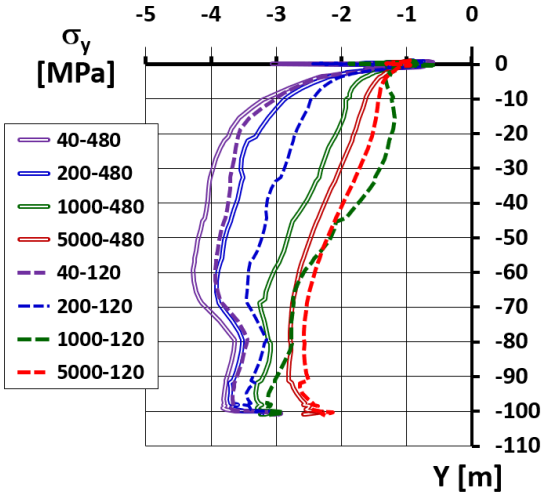

Figure 13. Wall height wise distribution of average vertical stresses.

From the point of view of providing compressive strength to the wall material, the unfavorable situation develops in the alternatives with the most deformed foundation (alternatives of series «a»). In this case, the compressive stresses reach approximately 4 MPa (Fig. 13), i.e. they exceed uniaxial compression strength of cast clay-cement concrete (approximately 2 MPa). However, from the experiments of a number of authors [25, 26] it is known that the strength of clay-cement increases significantly in the presence of lateral compression. Taking into account the influence of lateral compression effect, the strength of the CW can be ensured.

Evidently, a great risk for the wall workability is presented by tensile stresses in the bending zones. Tensile stresses at the section of CW conjugation with the rigid concrete apron are typical for the alternatives with soil foundation (alternative of series' "a", "b"). In these alternatives, the upper part of the joint between CW and the apron opens, thus, putting the seepage control contour at risk of tightness loss.

3.7. Stress state of the apron

Bending deformations are typical for SSS of the concrete apron. It is evident in Fig. 14 showing all the alternatives the distribution of horizontal stresses along the upstream and downstream parts of the face. Stresses are non-uniformly distributed along the thickness of the face.

The left and the right parts of the apron bend in different ways. The left part of the apron (approximately 4 m long) bends in upward direction, which is related to interaction with the wall (Fig. 14). The right part of the face bends downward.

The wall transfers compressive longitudinal (horizontal) force with intensity of approximately 1 MPa to the apron. However, bending deformations cause tensile stresses on the apron faces. Their value varies depending on the foundation rigidity.

At rigid (rock) foundation the stresses in the apron are small; its strength is provided with large safety factor. At deformed (soil) foundation, the tensile stresses are so great (Fig. 14), that they exceed concrete tensile strength. Moreover, in alternative “A.a”, compressive stresses exceed compressive strength of B30 grade concrete.

Thus, the concrete apron is the most vulnerable element of the composite seepage control facility of the dam on the deformed foundation. Besides, its high rigidity creates the unfavorable stress state in the head part of the wall.

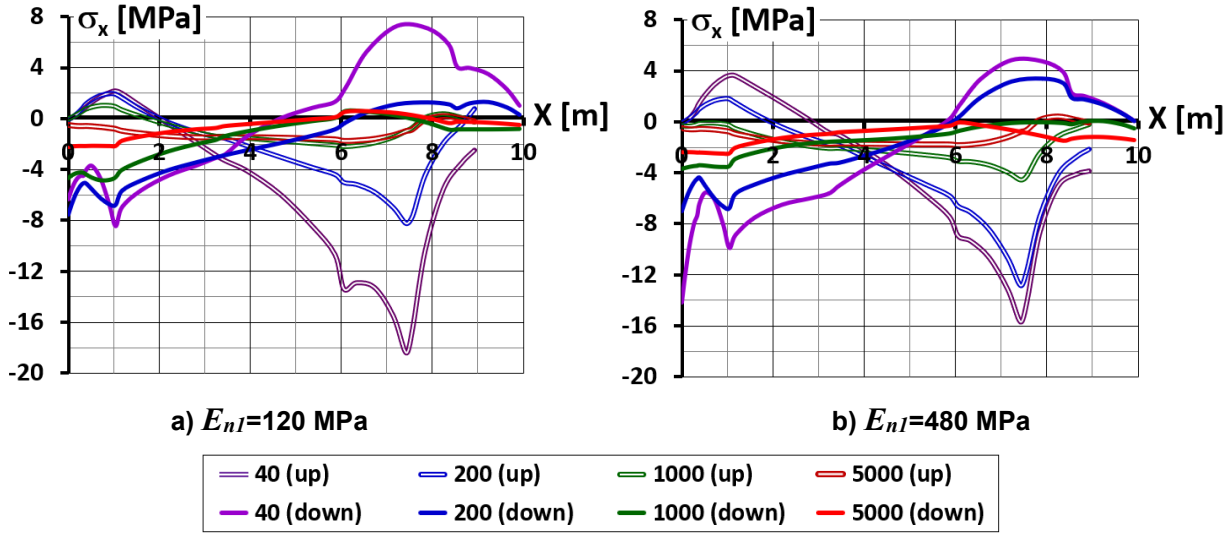

Figure 14. Distribution of average horizontal stresses lengthwise the apron on the upstream and downstream faces. In the designation there shown the value of deformation modulus of foundation (MPa) and the face.

4. Conclusion

Stress-strain state of CFRD, located on the deformed soil foundation drastically differs from SSS of the dam on the rigid rock foundation. Increase of the foundation deformation not only creates unfavorable SSS for the dam rockfill, but threatens the strength of the seepage control facility elements as well as tightness of their connections.

The degree of the foundation effect on the dam SSS depends on the thickness and deformation of the foundation soils as well as the width of the rock canyon. Nevertheless, one can distinguish several threats for the composite seepage control facility of CFRD, located on the deformed soil foundation:

1. The concrete face of the dam on soil foundation is subject to considerable compressive longitudinal forces. Taking into account the occurrence of possible stresses in the face from other factors (for example, from temperature effects), there is a risk of concrete compressive strength loss. Besides, if the foundation is by an order of magnitude more deformed than the rockfill, considerable tensile forces may also occur in the face leading to a probable loss of concrete tensile strength.
2. In spite of the fact that the seepage control wall is beyond the dam profile, it is subject to increased compressive stresses in vertical direction. Therefore, the wall material is at risk of compressive strength loss. In order to provide strength, it is recommended to choose the wall material with rigidity not more than 2–3 times greater than that the foundation soil.

3. Due to the wall thrust into the rigid concrete apron, there are two probable unfavorable effects for the tightness of the dam seepage control contour. First of all, it is formation of cracks in the wall head, secondly, it is opening of the joint between the apron and the wall. Wall connection to the apron should be designed as tight to prevent large displacements.
4. Concrete apron is the most vulnerable element of the composite seepage control facility. Due to great tensile stresses at bending there is a risk of crack formation in the apron. Designing the composite seepage control facility should include the measures for preserving the apron water tightness.

The problem of providing workability to the apron may be solved using several methods.

The first method is cutting the apron by transversal joints into 2–3 slabs. For example, the 10 m long apron of Aertash dam was cut into 3 slabs. The joints are located at a distance of 3 m and 6 m from the wall. This method provides effective decrease of tensile stresses. However, Fig. 14 shows that the joints are located not in the most dangerous sections, therefore, preventing of crack formation in the apron is not guaranteed.

The design of 92 m high dam Khao Laem (or Vajiralongkorn, Thailand) provided a concrete gallery above the apron, which permits grouting of the foundation and checking the condition of the apron.

The other method is possible. The author considered the alternative of the dam structural design, where the apron is made of asphalt concrete. It was shown that a decrease of the apron rigidity was favorable for the face SSS; strength of all the elements was provided. However, this method was tested only by the way of numerical modeling for one particular case.

References

1. Fu, Z., Chen, S., Ji, E. Practices in constructing high rockfill dams on thick overburden layers. Dam Engineering. 2019. Pp. 1–21. DOI: 10.5772/intechopen.78547
2. Wen, L., Qin, Y., Chai, J., Li, Y., Wang, X., Xu, Z. Behaviour of concrete-face rockfill dam on sand and gravel foundation. Proceedings of the Institution of Civil Engineers: Geotechnical Engineering. 2015. 168 (5). Pp. 439–456. DOI: 10.1680/geng.14.00103
3. Wen, L., Chai, J., Xu, Z., Qin, Y., Li, Y. Deformation and stress behaviours of concrete-face rockfill dam built on sand and gravel foundation. Shuili Fadian Xuebao/Journal of Hydroelectric Engineering. 2016. 35 (9). Pp. 63–77. DOI: 10.11660/slfdxb.20160908
4. Wen L., Chai J., Xu Z., Qin Y., Li Y. A statistical review of the behaviour of concrete-face rockfill dams based on case histories. Géotechnique. 2017. 68 (9). Pp. 749–771. DOI: 10.1680/jgeot.17.p.095
5. Wen L., Chai J., Xu Z., Qin Y., Li Y. A statistical analysis on concrete cut-off wall behaviour. Proceedings of the Institution of Civil Engineers — Geotechnical Engineering. 2018. 171 (2). Pp. 160–173. DOI: 10.1680/jgeen.17.00142
6. Sainov, M., Soroka, V., Gunasekaran, M. Combination of rockfill dam reinforced concrete face and seepage control wall in the foundation: stress-strain state. Construction of Unique Buildings and Structures. 2022. 99. 9902. DOI: 10.4123/CUBS.99.2
7. Lyapichev, Yu.P. Static and dynamic analyses of the heightening of concrete face gravel dam Limon. (Peru). Structural Mechanics of Engineering Constructions and Buildings. 2019. 15 (2). Pp.158–168.
8. Shen, T., Li, G.Y., Li, Y., Li, J., Feng, Y.L. Numerical analysis of joint types between toe slab and foundation of CFRD in alluvial deposit layer. Chinese Journal of Rock Mechanics and Engineering. 2005. 24. Pp. 2588–2592. DOI: 10.3321/j.issn:1000-6915.2005.14.030
9. Gan, L., Shen, Z.Z., Xu, L.Q. Long-term deformation analysis of the Jiudianxia concrete-faced rockfill dam. Arabian Journal for Science and Engineering. 2012. 39 (3). Pp. 1589–1598. DOI: 10.1007/s13369-013-0788-6
10. Sun, D.W., Wang, K.P., Yao, H.Q. 3D Finite Element Analysis on ChaHanWuSu CFRD Built on Thick Alluvium Deposits. Advanced Materials Research. 2011. 243–249. Pp. 4482–4487. DOI: 10.4028/www.scientific.net/AMR.243-249.4482
11. Wen, L., Chai, J., Xu, Z., Qin, Y., Li, Y. Monitoring and numerical analysis of behaviour of Miaojiaba concrete-face rockfill dam built on river gravel foundation in China. Computers and Geotechnics. 2017. 85. Pp. 230–248. DOI: 10.1016/j.compgeo.2016.12.018
12. Haselsteiner, R., Balat, V., Ersoy, B. The Optimization of the Design of a Concrete Faced Rockfill Dam by the Application of Sand-Gravel Fill Zones. Bundesanstalt für Wasserbau. 2011. Pp. 669–676.
13. Haselsteiner, R., Kaytan, E., Pamuk, R., Ceri, V. Seepage control design of the Arkun Dam in Turkey. International Journal on Hydropower and Dams. 2012. 19 (1). Pp. 90–95.
14. Sun, D., Deng, H., Tian, B., Li, N. Deformation and stress analysis of Dahe CFRD built on thick alluvium deposits. Chinese Journal of Geotechnical Engineering. 2008. 30 (3). Pp. 434–439.
15. Sainov, M.P., Soroka, V.B. Enhancement of a seepage control facility of an earth-filled dam that has a concrete face and a cutoff wall. Stroitel'stvo: nauka i obrazovanie [Construction: Science and Education]. 2022. 12(1). 2. DOI: 10.22227/2305-5502.2022.1.2
16. Materon, B., Resende, F. Construction Innovations for the Itapebi CFRD. International Journal on Hydropower & Dams. 2001. 8(5). Pp. 66–70.
17. Zhang, G., Zhang, J.-M. Modeling of low-cement extruded curb of concrete-faced rockfill dam. Canadian Geotechnical Journal. 2011. 48 (1). Pp. 89–97.
18. Cheng, P., De-fa, G.U.O., Qing, W. Application of extrusion-sidewall technology to the project of rock fill dam with face slab. 2008. Pp. 201–203.
19. Pinto, N.L.D.S. Questions to ponder on designing very high CFRDs. International Journal on Hydropower and Dams. 2001. 8 (5). Pp. 61–65.

20. Mirghasemi, A.A., Pakzad, M., Shadravan, B. The world's largest cutoff wall at Karkheh dam. International Journal on Hydropower and Dams. 2005. 12 (2). Pp. 2–6.
21. Faridmehr, I., Yazdanipour, M.R., Jokar, M.J., Ozbakkaloglu, T. Construction and Monitoring of Cement/Bentonite Cutoff Walls: Case Study of Karkheh Dam, Iran. Studia Geotechnica et Mechanica. 2019. (July). Pp. 1–16. DOI: 10.2478/sgem-2019-0019
22. Grishin, V.A., Deryugin, L.M. Experience in the use of bentonite-cement concrete for repairing the core of the earthfill dam of Kureiskaya HPP. Power Technology and Engineering. 2006. 40 (2). Pp. 90–95.
23. Arici, Y. Investigation of the cracking of CFRD. face plates. Computers and Geotechnics. 2011. 38 (7). Pp. 905–916. DOI: 10.1016/j.compgeo.2011.06.004
24. Sainov, M.P. Strength of ultra-high rockfill dam concrete face. Magazine of Civil Engineering. 2021. 101 (1). 10113. DOI: 10.18720/MCE.101.13
25. Rasskazov, L.N., Radzinskii, A.V., Sainov, M.P. Strength and Deformability of Clay-Cement Concrete in a Complex Stress State. Power Technology and Engineering. 2015. 48(5) Pp. 361-365. DOI: 10.1007/s10749-015-0534-1
26. Razavi S.-K., Hajialilue-Bonab M., Pak A. Design of a Plastic Concrete Cutoff Wall as a Remediation Plan for an Earth-Fill Dam Subjected to an Internal Erosion. International Journal of Geomechanics. 2021. 21(5): 04021061. DOI: 10.1061/(ASCE)GM.1943-5622.000199

Information about authors

Mikhail Sainov, *Doctor of Technical Sciences*
ORCID: https://orcid.org/0000-0003-1139-3164
E-mail: mp_sainov@mail.ru

Received 13.02.2023. Approved after reviewing 01.12.2023. Accepted 11.12.2023.